Transplantation and tolerance

Basic

Research Article

Glucocorticoids delivered by inorganic–organic hybrid nanoparticles mitigate acute graft-versus-host disease and sustain graft-versus-leukemia activity

Tina K. Kaiser*[1], Hu Li*[1], Laura Roßmann[1], Sybille D. Reichardt[1], Hanibal Bohnenberger[2], Claus Feldmann[3] and Holger M. Reichardt[1] (ID)

[1] Institute for Cellular and Molecular Immunology, University Medical Center Göttingen, Göttingen, Germany
[2] Institute of Pathology, University Medical Center Göttingen, Göttingen, Germany
[3] Institute of Inorganic Chemistry, Karlsruhe Institute of Technology, Karlsruhe, Germany

Glucocorticoids (GCs) are widely used to treat acute graft-versus-host disease (aGvHD) due to their immunosuppressive activity, but they also reduce the beneficial graft-versus-leukemia (GvL) effect of the allogeneic T cells contained in the graft. Here, we tested whether aGvHD therapy could be improved by delivering GCs with the help of inorganic–organic hybrid nanoparticles (IOH-NPs) that preferentially target myeloid cells. IOH-NPs containing the GC betamethasone (BMP-NPs) efficiently reduced morbidity, mortality, and tissue damage in a totally MHC mismatched mouse model of aGvHD. Therapeutic activity was lost in mice lacking the GC receptor (GR) in myeloid cells, confirming the cell type specificity of our approach. BMP-NPs had no relevant systemic activity but suppressed cytokine and chemokine gene expression locally in the small intestine, which presumably explains their mode of action. Most importantly, BMP-NPs delayed the development of an adoptively transferred B cell lymphoma better than the free drug, although the overall incidence was unaffected. Our findings thus suggest that employing IOH-NPs could diminish the risk of relapse associated with GC therapy of aGvHD patients while still allowing to efficiently ameliorate the disease.

> 🖥 Additional supporting information may be found online in the Supporting Information section at the end of the article.

Introduction

Glucocorticoids (GCs) are recommended for the initial treatment of acute graft-versus-host disease (aGvHD), since they potently suppress the underlying immune response by regulating the activity of T cells, macrophages and other cell types [1,2]. However, their broad range of target cells also entails many side-effects, including off-target effects such as the induction of muscle atrophy, osteoporosis, hypertension, and dysglycemia [2–5]. Moreover, GCs also evoke on-target effects related to their

*These authors contributed equally to the work.

immunosuppressive activity, i.e., an increased susceptibility to infections and an impaired antitumor response after HSC transplantation (HSCT), commonly known as the graft-versus-leukemia (GvL) effect. Hence, new strategies aimed to reduce adverse effects of GCs while retaining their beneficial activities are needed and may improve the tolerability of this widely used therapeutic regimen.

HSCT is often the last option to treat hematopoietic malignancies that do not respond to other conventional therapies [6,7]. The conditioning regimen applied in patients undergoing HSCT causes tissue damage and initiates an innate immune response, while the allogeneic T cells contained in the graft recognize major and minor histocompatibility complex antigens of the recipient as foreign and cause an adaptive immune response. Eventually, macrophages and T cells produce pro-inflammatory cytokines and mediators that attack target organs such as the small intestine, liver, and skin, an effect that is responsible for the majority of clinical symptoms observed in aGvHD patients. Application of synthetic GCs such as prednisolone is the standard first-line therapy of this disease [2,8]. However, there is a considerable number of aGvHD patients that do not respond to GCs or become resistant during treatment, in which case second-line therapies are initiated such as anti-thymocyte globulin or targeted inhibitors of TNF-α activity. Importantly, most immunosuppressive therapies including GCs compromise the GvL effect of the graft as they suppress T cell functions that are necessary to eradicate residual malignant cells. Efficient amelioration of aGvHD and the concomitant prevention of a relapse is therefore difficult to achieve.

Studies performed in GC resistant mouse models revealed that the deletion of the GC receptor (GR) either in allogeneic T cells or recipient myeloid cells resulted in a severely aggravated aGvHD regardless of which of the two cell types was refractory to the activity of endogenous GCs [9,10]. However, the underlying mechanisms were different in both models. GC resistance of allogeneic T cells resulted in an increased cytotoxicity leading to massive tissue damage in the small intestine and other target organs, accompanied by a broadly altered gene expression profile not only affecting T cells but also macrophages and intestinal epithelial cells [11]. In contrast, GC resistance of recipient myeloid cells had only little effect on gene expression but rather caused a severe cytokine release syndrome that endogenous GCs failed to control. In another study, prednisolone treatment of aGvHD in a haploidentical mouse model was found to reduce the expression of various cytokines, chemokines, and adhesion molecules, an effect that was most prominent in the inflamed intestine [12]. These findings suggest that GCs exert their beneficial activity via different cell types and mechanisms, and that addressing only some of them might be sufficient to ameliorate the disease.

GCs reach all tissues with essentially the same efficacy and then passively diffuse into cells across the plasma membrane. Encapsulation of GCs in nanostructures, however, alters both tissue distribution and uptake efficacy, and thereby allows a more targeted drug delivery [13]. In addition, nanomaterial preferentially localizes to inflamed tissues due to their extravasation through leaky vasculature and subsequent inflammatory cell-mediated sequestration (ELVIS), which is a favorable mechanism in the treatment of inflammatory diseases [14,15]. Previous publications reported that GCs encapsulated in PEGylated liposomes preferentially acted on macrophages and monocytes and improved the treatment of autoimmune diseases [16,17]. Polymer–drug conjugates and polymeric micelles containing GCs were also found to exert potent anti-inflammatory activity in mice while eliciting less side effects in bone [18–21]. Another recently introduced option are inorganic–organic hybrid nanoparticles (IOH-NPs) with the chemical composition $[ZrO]^{2+}[(BMP)_{0.9}(FMN)_{0.1}]^{2-}$ (designated BMP-NPs). They are made of betamethasone phosphate (BMP), a synthetic GC derivative frequently used in the clinic, the fluorescent dye flavin mononucleotide (FMN), and the inorganic compound zirconium oxide. IOH-NPs have a hydrodynamic diameter of 30–40 nm and are stable in suspension [22]. They are efficiently engulfed by macrophages, to a lesser degree by fibroblasts, epithelial cells, and myoblasts, and hardly at all by T and B cells [23]. The uptake of IOH-NPs proceeds via macropinocytosis, followed by their trafficking to the lysosomal compartment and the release of the drug. Magnetic resonance imaging of mice revealed a rapid dissemination of IOH-NPs to abdominal organs including the small intestine after intraperitoneal injection, and an efficient uptake of IOH-NPs by myeloid but not T cells in the lamina propria [23]. In addition, BMP-NPs potently ameliorated EAE, a mouse model of MS [22], suggesting that the new nanoformulation might also be suitable for the treatment of aGvHD. Importantly, therapeutic efficacy of BMP-NPs in the EAE model was fully dependent on the modulation of myeloid cells, whereas the activity of GCs encapsulated in PEGylated liposomes was less specific [16], suggesting that IOH-NPs might have superior features compared to other nanoformulations.

Here, we set out to test the activity and mechanism of BMP-NPs using an aGvHD/GvL mouse model. We found that they efficiently mitigated clinical and histological hallmarks of aGvHD and delayed the development of an adoptively transferred B cell lymphoma better than the free drug. These findings recommend BMP-NPs as an alternative first-line therapy of aGvHD.

Results

BMP-NPs reduce mortality and morbidity in an aGvHD mouse model

A totally MHC mismatched aGvHD mouse model was used to assess the therapeutic efficacy of BMP-NPs. In this model, transplantation of bone marrow (BM) cells and splenic T cells from C57BL/6 mice into irradiated BALB/c mice causes rapidly aggravating clinical symptoms during the first 6–8 days, followed by a transient amelioration and a subsequent flare-up of the disease that eventually results in the death of the animals (Fig. 1A).

All mice receiving only BM cells survived until the end of the experiment. In contrast, most of the mice transplanted with BM and T cells and injected with the vehicles (PBS or empty
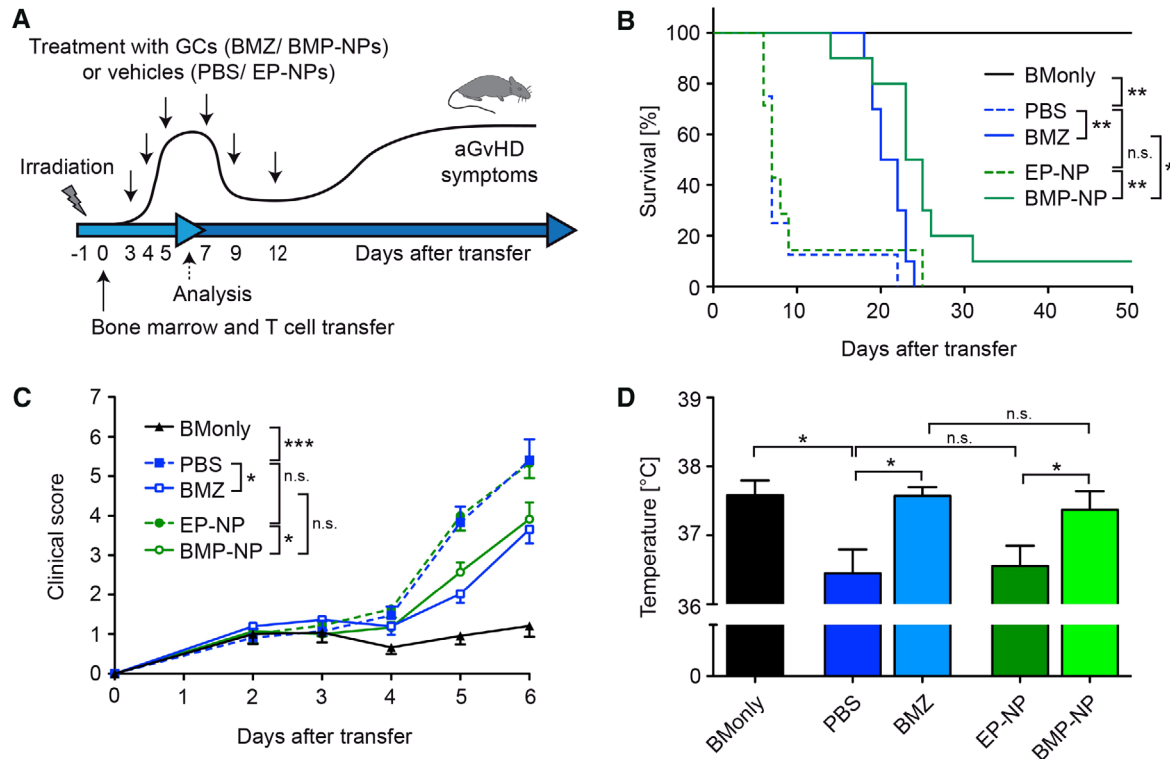
Figure 1. Impact of GC treatment on mortality and clinical features of aGvHD. BALB/c mice were irradiated and subsequently transplanted with BM and purified T cells from C57BL/6 mice. In the case of short-term experiments (C and D), treatment with GCs (BMZ or BMP-NP) or vehicles (PBS or EP-NP) was performed at days 3, 4, and 5. In the case of long-term experiments (B), mice were additionally treated at days 7, 9, and 12. Mice receiving only BM cells served as a control. (A) Schematic representation of aGvHD experiments and the therapeutic regimen. (B) Survival of mice based on the applying ethical criteria was monitored for 50 days. $N = 4$ (BMonly), $N = 8/10$ (PBS/BMZ), $N = 7/10$ (EP/BMP-NP); data were pooled from two experiments. Statistical analysis was done by Log-rank Mantel–Cox test. (C) Development of clinical scores of mice until day 6. $N = 12$ (BMonly), $N = 21/22$ (PBS/BMZ), $N = 23/23$ (EP/BMP-NP); data were pooled from five experiments. Statistical analysis refers to day 6. (D) Body temperature of mice at day 6. $N = 6$ (BMonly), $N = 10/12$ (PBS/BMZ), $N = 9/12$ (EP/BMP-NP); data were pooled from three experiments. Values in panels (C) and (D) are depicted as the mean ± SEM and were analyzed using a one-way ANOVA followed by a Newman–Keuls Multiple Comparison test. Levels of significance are $*p < 0.05$; $**p < 0.01$; $***p < 0.001$; n.s., non-significant. The indicated sample size (N) refers to the total number of individual mice analyzed in each experimental group.

IOH-NPs without the drug, designated EP-NPs) had to be sacrificed until day 10 for ethical reasons (Fig. 1B). When we treated mice six times during the first 2 weeks (at days 3, 4, 5, 7, 9, and 12) with free betamethasone (BMZ) or BMP-NPs, survival was significantly prolonged compared to the respective vehicle-treated mice (Fig. 1B). Although BMP-NPs delayed the attainment of the ethical abort criteria more efficiently than BMZ, the difference between both treatment groups was small (Fig. 1B).

To evaluate the impact of GC therapy on the severity of clinical symptoms in the initial phase of the disease, we treated the mice at days 3, 4, and 5 and followed aGvHD progression until day 6. Mice receiving only PBS or EP-NPs after BMT cell transfer showed increasing signs of diarrhea, abdominal pain, and weight loss and approached the applying abort criteria at the end of the observation period (Fig. 1C). Treatment of mice with BMZ or BMP-NPs after BMT cell transfer significantly reduced clinical symptoms, although to a similar extent in both cases (Fig. 1C). Control mice receiving only BM cells showed only mild symptoms caused by the irradiation regimen. It is worth mentioning that mice of the two vehicle-treated groups also showed a drop in body tempera-

ture compared to mice receiving only BM cells, an effect that was prevented by injecting BMZ as well as BMP-NPs (Fig. 1D). We conclude that both GC formulations ameliorate clinical symptoms in the early phase of aGvHD with similar efficacy, although the activity of BMP-NPs appears to be more sustained as indicated by the slightly prolonged survival of mice from this group (Fig. 1B).

Therapeutic activity of BMP-NPs correlates with tissue damage in the small intestine

Many of the clinical symptoms observed in aGvHD such as diarrhea and abdominal pain can be attributed to the extensive tissue damage caused by the allogeneic T cell response at target sites such as the small intestine. Hence, we determined pathological alterations and immune cell infiltration in the small intestine by histological staining and immunohistochemistry around the first peak of the disease at day 6. The histopathological score of mice treated with PBS or EP-NPs was increased in comparison to control mice whereas the number of goblet cells was reduced (Figs. 2A
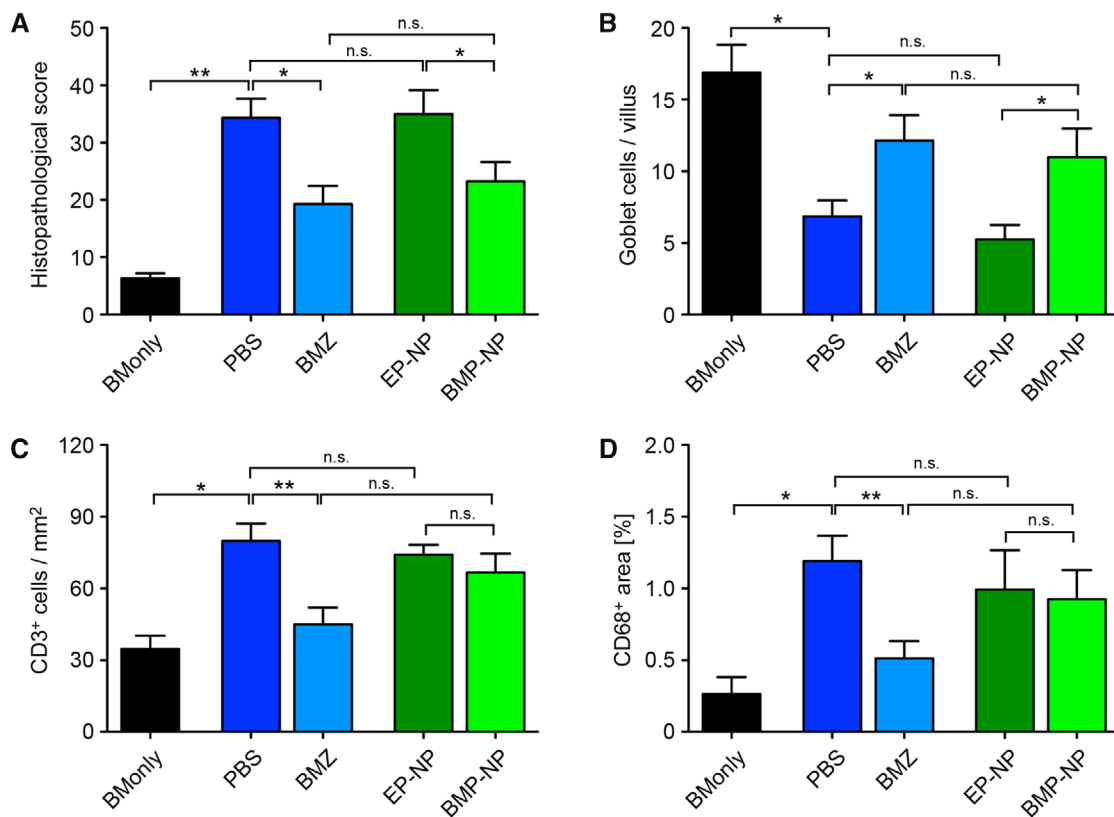
Figure 2. Histological and immunohistochemical evaluation of the small intestine in the early phase of aGvHD after GC treatment. BALB/c mice were irradiated and subsequently transplanted with BM and purified T cells from C57BL/6 mice. Treatment with GCs (BMZ or BMP-NP) or vehicles (PBS or EP-NP) was performed at days 3, 4, and 5; mice receiving only BM cells served as a control. Biopsies of the small intestine were collected at day 6. (A) Histopathological scores obtained by assessment of H&E stained sections of the small intestine. $N = 4$ (BMonly), $N = 9/10$ (PBS/BMZ), $N = 9/12$ (EP/BMP-NP). (B) Goblet cell numbers per villus determined in PAS stainings of sections of the small intestine. $N = 4$ (BMonly), $N = 11/11$ (PBS/BMZ), $N = 8/10$ (EP/BMP-NP). (C) Numbers of CD3$^+$ cells per square millimeter as determined by counting of immunoreactive cells in sections of the small intestine. $N = 4$ (BMonly), $N = 11/11$ (PBS/BMZ), $N = 9/12$ (EP/BMP-NP). (D) Quantification of CD68$^+$ cells by measuring the percentage of the area covered by immunoreactive cells in sections of the small intestine using ImageJ software. $N = 4$ (BMonly), $N = 8/8$ (PBS/BMZ), $N = 9/12$ (EP/BMP-NP). Data in all panels were pooled from four experiments. All values are depicted as mean $\pm$ SEM; statistical analyses were performed by one-way ANOVA followed by a Newman–Keuls multiple comparison test. Levels of significance are $^*p < 0.05$; $^{**}p < 0.01$; $^{***}p < 0.001$; n.s., non-significant. The indicated sample size (N) refers to the total number of individual mice analyzed in each experimental group.

and B, and 3). More specifically, the villi in the small intestine were severely damaged, which was accompanied by the presence of apoptotic cells, edema, and signs of inflammation (Fig. 3). BMZ and BMP-NP treatment ameliorated the symptoms as reflected by lower histopathological scores and increased goblet cell numbers (Fig. 2A and B). However, there was no difference between both treatment groups. Immunohistochemical stainings were performed to take a closer look at the infiltrating leukocytes (Fig. 3). The numbers of CD3$^+$ T cells and CD68$^+$ myeloid cells were significantly increased in aGvHD mice receiving vehicles compared to BMonly controls (Fig. 2C and D). BMZ treatment prevented the infiltration of these immune cells into the small intestine, which is in line with the improved histopathological scores in this experimental group (Fig. 2A–D). Surprisingly, BMP-NPs neither reduced the number of T cells nor myeloid cells in the small intestine despite their previously demonstrated ability to ameliorate tissue damage and clinical symptoms (Fig. 2A–D). Collectively, our findings indicate that both GC formulations impact the disease course

by preserving the tissue integrity of the small intestine and presumably other aGvHD target organs. BMZ achieves this at least in part by interfering with immune cell trafficking while BMP-NPs must employ a different mechanism.

Unaltered T cell and myeloid cell composition in the small intestine after BMP-NP therapy

Although our immunohistochemical analysis revealed that BMP-NP treatment did not impact the number of the two major immune cell subsets in the small intestine, it was still conceivable that their composition was altered. Namely, CD4$^+$ and CD8$^+$ T cells fulfill different functions in the pathogenesis of aGvHD, and myeloid cells can adopt an inflammatory Ly6C^{high} or resident Ly6C^{low} phenotype. To determine whether BMP-NPs alter the subtype composition of immune cells in target organs, we isolated the cells from the lamina propria of the small intestine and analyzed them
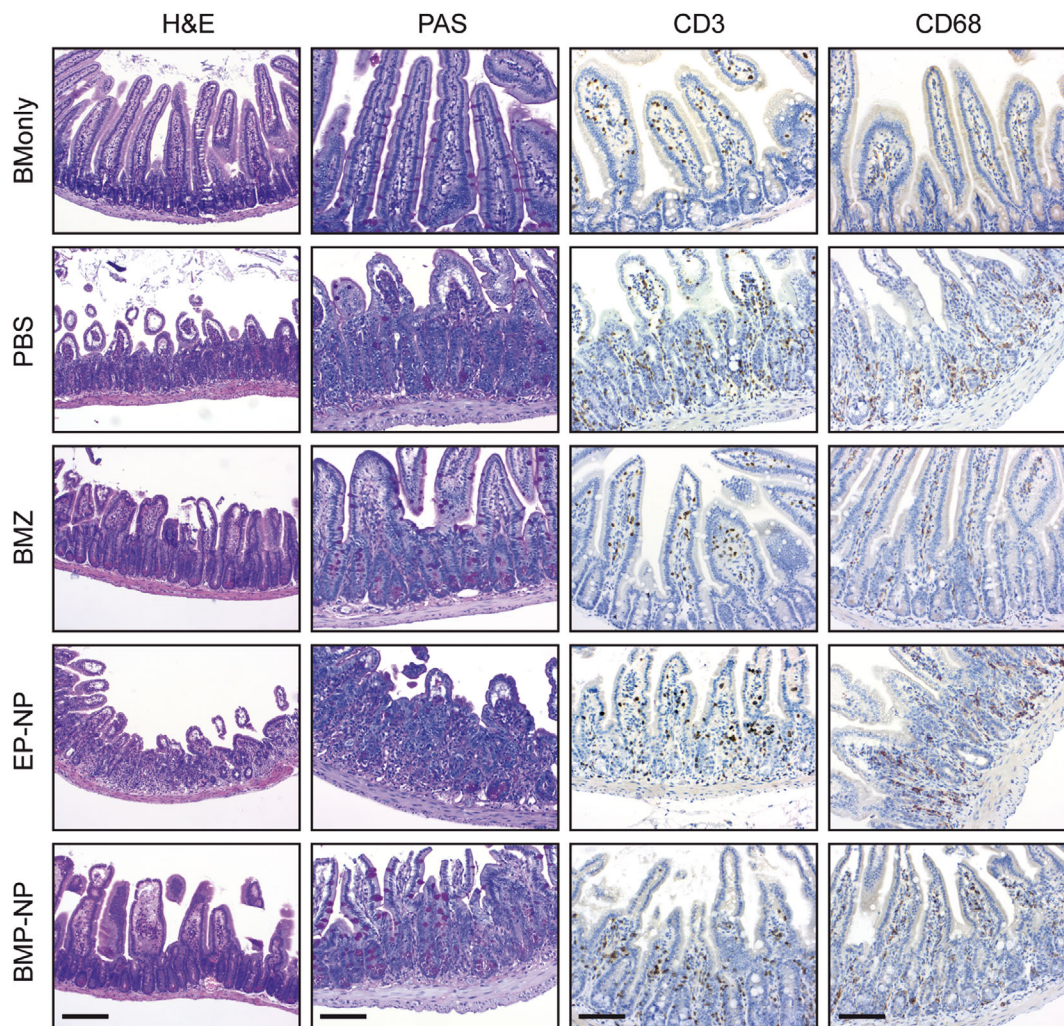
Figure 3. Representative photomicrographs of the small intestine in the early phase of aGvHD after GC treatment. BALB/c mice were irradiated and subsequently transplanted with BM and purified T cells from C57BL/6 mice. Treatment with GCs (BMZ or BMP-NP) or vehicles (PBS or EP-NP) was performed at days 3, 4, and 5; mice receiving only BM cells served as a control. The small intestine was collected at day 6 from mice of all five experimental groups and sections were stained with H&E or by PAS reaction. Additional sections were incubated with antibodies recognizing either CD3 or CD68 to visualize T cells and myeloid cells, respectively. Representative microphotographs aquired at a 100× (H&E) or 200× (PAS, CD3, CD68) magnification (from the experiments summarized in Fig. 2) are depicted. Size bars: 200 μm (H&E), and 100 μm (PAS, CD3, CD68).

by flow cytometry. The percentage of CD4$^+$ T cells was reduced in aGvHD mice treated with PBS or EP-NPs compared to control mice and the percentage of CD8$^+$ T cells was increased, but neither treatment with BMZ nor BMP-NPs reversed these alterations (Fig. 4A and B). In addition, the percentage of mono-cytes/macrophages with an Ly6C^{high} inflammatory phenotype was increased in aGvHD mice treated with PBS or EP-NPs in comparison to control mice and the percentage of myeloid cells with a Ly6C^{low} resting phenotype was concomitantly decreased (Fig. 4C and D). BMZ reversed the observed shift in subtype composition, either by interfering with the de novo recruitment of inflammatory monocytes/macrophages to the small intestine or by polarizing them toward an anti-inflammatory phenotype in situ. Importantly, the composition of myeloid cells in the small intestine was unaffected by BMP-NPs, indicating that GCs delivered via IOH-NPs act in a different manner than the free drug (Fig. 4C and D).

Myeloid cells are essential targets of the therapeutic activity of BMP-NPs

Previous studies indicated that IOH-NPs were preferentially taken up by myeloid cells such as macrophages, for which reason GR^{lysM} mice lacking the GR in this cell type were refractory to BMP-NP therapy in a mouse model of MS [22]. To test whether modulation of myeloid cells was crucial for the BMP-NPs' therapeutic efficacy in aGvHD as well, clinical symptoms and pathological hallmarks were analyzed in GR^{flox} and GR^{lysM} mice at day 6 after aGvHD induction. GR^{flox} mice injected with EP-NPs developed severe clin-ical symptoms and a reduced body temperature, and both fea-tures were mitigated by BMP-NP treatment (Fig. 5A and B). In contrast, BMP-NPs did not show any therapeutic activity in GR^{lysM} mice as reflected by their high clinical score and low body tem-perature, which were both undistinguishable from mice receiving
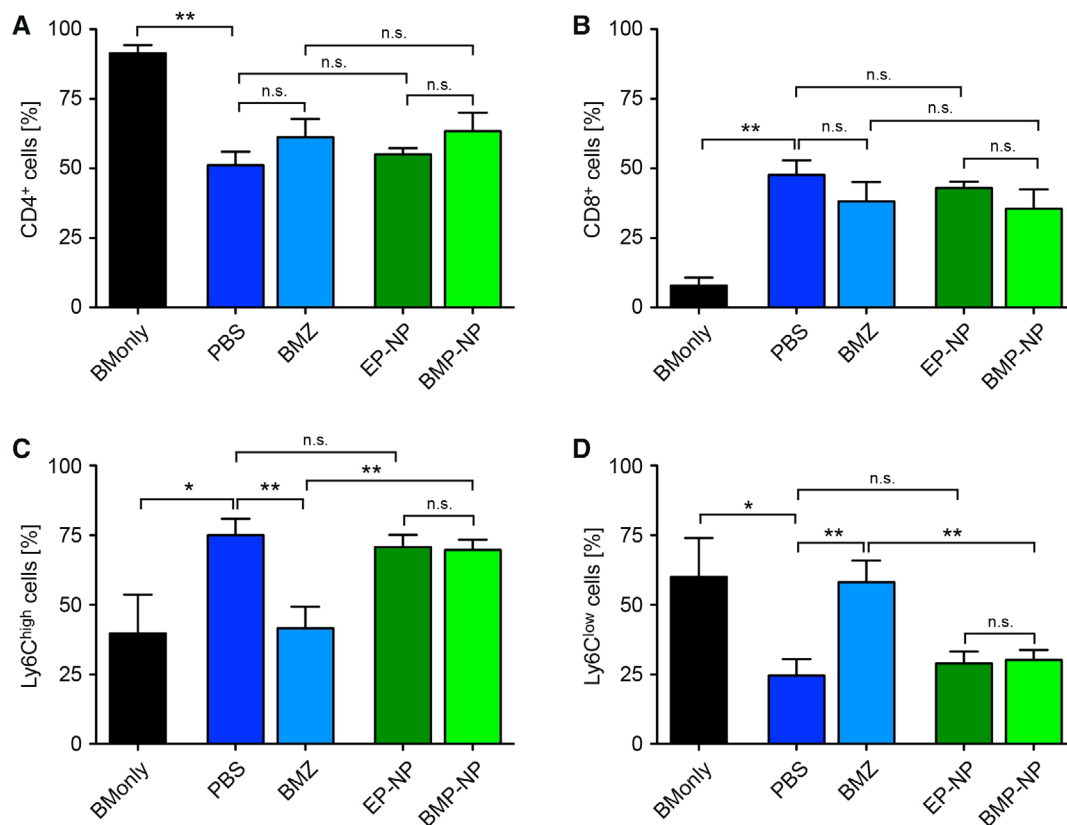
Figure 4. Flow cytometric analysis of cells isolated from the lamina propria of the small intestine in the early phase of aGvHD after GC treatment. BALB/c mice were irradiated and subsequently transplanted with BM and purified T cells from C57BL/6 mice. Treatment with GCs (BMZ or BMP-NP) or vehicles (PBS or EP-NP) was performed at days 3, 4, and 5; mice receiving only BM cells served as a control. Lamina propria cells were prepared from the small intestine at day 6 and analyzed by flow cytometry. (A and B) Percentages of CD4+ and CD8+ cells among CD3+ T cells (gated for live cells and singlets). $N = 3$ (BMonly), $N = 8/5$ (PBS/BMZ), $N = 5/6$ (EP/BMP-NP); data were pooled from three experiments. (C and D) Percentages of Ly6C^{high} and Ly6C^{low} cells among CD11b+ Ly6G^{low} monocytes/macrophages (gated for live cells and singlets). $N = 4$ (BMonly), $N = 7/5$ (PBS/BMZ), $N = 5/6$ (EP/BMP-NP); data were pooled from three experiments. All values are depicted as mean ± SEM; statistical analyses were performed by one-way ANOVA followed by a Newman–Keuls multiple comparison test. Levels of significance are *$p < 0.05$; **$p < 0.01$; ***$p < 0.001$; n.s., non-significant. The indicated sample size (N) refers to the total number of individual mice analyzed in each experimental group. The gating strategies are illustrated in Supporting Information Figs. 1 and 2.

EP-NPs (Fig. 5A and B). A similar observation was made concerning tissue damage in the small intestine. GR^{flox} mice injected with EP-NPs had a high histopathological score and a low number of goblet cells, both of which were reversed by BMP-NP treatment (Fig. 5C and D). In contrast, BMP-NP treatment had no effect on tissue damage in GR^{lysM} mice, indicating that GCs delivered with the help of IOH-NPs ameliorate aGvHD by acting on myeloid cells.

Systemic cytokine levels are unaffected by GC therapy of aGvHD

GR deficiency in myeloid cells was previously found to aggravate aGvHD due to the inability of endogenous GCs to counteract systemic cytokine secretion [9]. Thus, it was conceivable that therapeutic GCs also acted by reducing pro-inflammatory cytokine and chemokine levels in the serum. Induction of aGvHD led to increased concentrations of TNF-α, IL-6, CCL-2, and IFN-γ in the

circulation at day 6, although to a different degree. Surprisingly, serum levels were similar regardless of whether the mice were treated with GCs in either formulation or whether they received the respective vehicles (Fig. 6). This observation indicates that therapeutic GCs, in contrast to endogenous hormones, have only little effect on steady-state systemic cytokine and chemokine levels despite being able to ameliorate aGvHD.

BMP-NPs repress local gene expression of cytokines and chemokines in the small intestine

Nanosized drug formulations preferentially localize to inflamed tissues as a consequence of the ELVIS mechanism [14, 15]. In addition, it was found that IOH-NPs accumulate in the small intestine after intraperitoneal injection into mice and that they are predominantly taken up by myeloid cells [22,23]. Hence, it was conceivable that BMP-NPs locally regulate the function of monocytes and macrophages in aGvHD target organs, although their
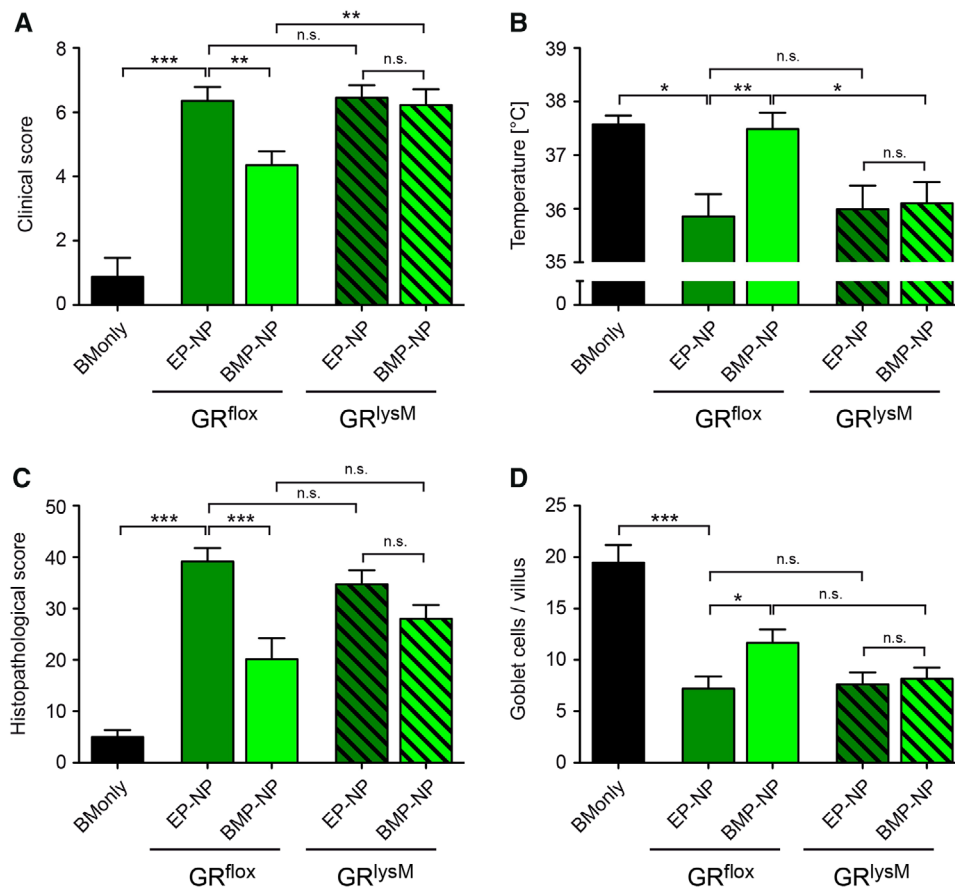
Figure 5. Impact of GC treatment on clinical and histological features of aGvHD in the GR^{lysM} mouse model. GR^{flox} and GR^{lysM} mice on a BALB/c background were irradiated and then transplanted with BM and purified T cells from C57BL/6 WT mice. Treatment with BMP-NPs or EP-NPs was performed at days 3, 4, and 5; mice receiving only BM cells served as a control. (A) Clinical scores of mice at day 6. $N = 4$ (BMonly), $N = 7/10$ (GR^{flox}; EP/BMP-NP), $N = 10/9$ (GR^{lysM}; EP/BMP-NP). (B) Body temperature of mice at day 6. $N = 4$ (BMonly), $N = 7/10$ (GR^{flox}; EP/BMP-NP), $N = 10/9$ (GR^{lysM}; EP/BMP-NP). (C) Histopathological scores obtained by assessment of H&E stained sections of the small intestine collected at day 6. $N = 4$ (BMonly), $N = 7/7$ (GR^{flox}; EP/BMP-NP), $N = 8/9$ (GR^{lysM}; EP/BMP-NP). (D) Goblet cell numbers per villus as determined in PAS stainings of sections of the small intestine collected at day 6. $N = 3$ (BMonly), $N = 7/8$ (GR^{flox}; EP/BMP-NP), $N = 7/8$ (GR^{lysM}; EP/BMP-NP). Data were pooled from three experiments. Values are depicted as the mean ± SEM and were analyzed using a one-way ANOVA followed by a Newman–Keuls multiple comparison test. Levels of significance are $^*p < 0.05$; $^{**}p < 0.01$; $^{***}p < 0.001$; n.s., non-significant. The indicated sample size (N) refers to the total number of individual mice analyzed in each experimental group.

number was unaffected by BMP-NPs. To address this issue, we isolated RNA from the small intestine at day 6 and analyzed it by quantitative RT-PCR. Induction of aGvHD caused an elevated gene expression of *Tnfa*, *Il6*, *Ccl2*, *Il10*, *Il2*, and *Ifng* in mice receiving vehicles compared to BMonly control mice (Fig. 7). Importantly, treatment with BMZ or BMP-NPs both reduced the mRNA levels of all genes, although significance was missed for two of them (Fig. 7). We conclude that IOH-NPs locally act in aGvHD target organs, where the encapsulated GCs regulate gene expression in immune cells after their engulfment.

The GvL activity is improved in mice receiving BMP-NPs compared to free GCs

The allogeneic T cells contained in the graft are not only responsible for inducing aGvHD but also help eliminating residual lymphoma cells. Since the latter activity is compromised by any

type of immunosuppressive therapy including GCs, relapses are a risk in patients receiving HSCT. Since BMP-NPs selectively act on myeloid cells while being hardly taken up by T cells [22,23], we hypothesized that this therapeutic regimen might retain the beneficial GvL effect of the graft. To address this issue, we used a combined aGvHD/GvL mouse model (Fig. 8A). Syngeneic Bcl$_1$ lymphoma cells were injected into irradiated BALB/c mice followed by BMT cell transplantation. Control mice receiving only Bcl$_1$ cells developed a lymphoma characterized by splenomegaly and a high percentage of malignant cells in the peripheral blood, on which basis the mice were sacrificed for ethical reasons between day 22 and 27 (Fig. 8B and C). Additional transplantation of BMT cells and injection of the vehicles PBS or EP-NPs resulted in the death of all mice before day 10 due to a severe aGvHD (Fig. 8B). However, when we treated mice receiving Bcl$_1$ and BMT cells with either of the two GC formulations BMZ or BMP-NPs, survival was significantly prolonged compared to all other groups (Fig. 8B). Furthermore, we observed a slight tendency that mice treated with
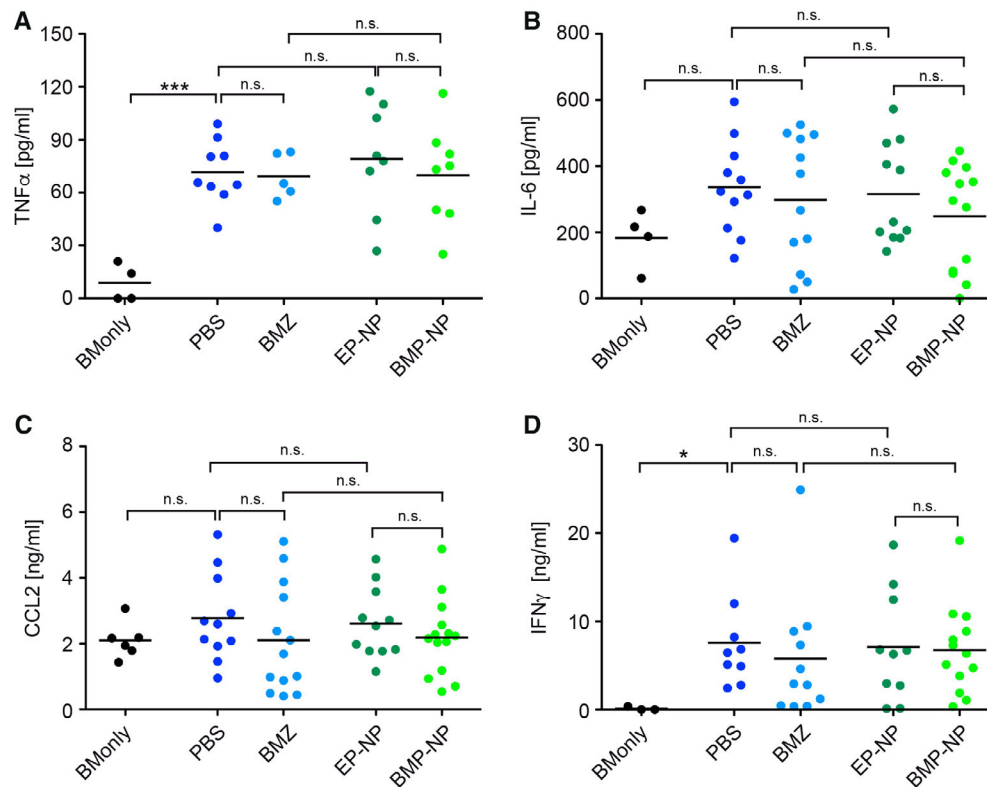
Figure 6. Cytokine serum levels in the early phase of aGvHD after GC treatment. BALB/c mice were irradiated and then transplanted with BM and purified T cells from C57BL/6 mice. Treatment with GCs (BMZ or BMP-NP) or vehicles (PBS or EP-NP) was performed at days 3, 4, and 5; mice receiving only BM cells served as a control. Blood samples were collected by cardiac puncture at day 6 and serum levels of (A) TNF-α, (B) IL-6, (C) CCL2, and (D) IFN-γ were determined by ELISA. $N = 3–6$ (BMonly), $N = 9–11$ (PBS), $N = 5–13$ (BMZ), $N = 7–11$ (EP-NP), $N = 8–14$ (BMP-NP); data were pooled from three experiments. Dots correspond to values obtained in individual mice, horizontal lines indicate the mean value. Data were analyzed using a one-way ANOVA followed by a Newman–Keuls multiple comparison test; levels of significance are $*p < 0.05$; $***p < 0.001$; n.s., non-significant. The indicated sample size (N) refers to the total number of individual mice analyzed in each experimental group.

BMP-NPs survived longer than those ones receiving BMZ, which is in line with our data obtained in the pure aGvHD model (Fig. 1B). Altogether, these findings led us to conclude that BMP-NPs also have therapeutic efficacy in a combined aGvHD/GvL model.

To compare the impact of BMZ and BMP-NPs on GvL activity more directly, we monitored the abundance of lymphoma cells in the circulation. Mice receiving only Bcl$_1$ cells showed a rapid expansion of the lymphoma cells in the blood starting around day 20. In contrast, Bcl$_1$ cells accumulated much later in mice additionally receiving BMT cells followed by GC therapy due to the GvL activity associated with the graft (Fig. 8C). Importantly, lymphomagenesis in mice treated with BMP-NPs was significantly delayed compared to mice receiving free BMZ, albeit the overall incidence was largely similar in both groups (Figs. 8C and 9). These findings suggest that the GvL activity is improved when GCs are applied via IOH-NPs, resulting in a retarded development of a B lymphoma.

Discussion

GCs remain the first-line therapy of choice to treat aGvHD, although overall response rates are unsatisfactory [2]. Further-

more, there is a variety of adverse effects that can accompany GC therapy such as myopathy, osteoporosis, diabetes, dysglycemia, hypertension, and infections. However, among the second-line therapies that are available for the treatment of aGvHD, there is also none which has been proven superior to another [8], for which reason efforts are still being made to improve the efficacy and tolerability of GCs. One clinical trial investigated whether a combination of methylprednisolone with daclizumab, a humanized monoclonal anti-CD25 antibody, improved therapeutic success, but survival of patients treated with both drugs was even diminished [24]. Noteworthy, deaths were related to both aGvHD and a relapse of the underlying disease. Daclizumab prevents the proliferation and differentiation of alloreactive T cells including those ones recognizing residual malignant cells [25]. Hence, it presumably compromised the GvL effect, resulting in an enhanced relapse rate. Since daclizumab also depletes regulatory T cells, the combination therapy additionally enhanced aGvHD mortality [26,27]. These findings highlight that new strategies are needed that prevent aGvHD without addressing T cells. This could be achieved, for instance, by targeting GCs to myeloid cells with the help of nanoformulations [13]. PEGylated liposomes, polymer–drug conjugates, polymeric micelles, and hybrid nanoparticles have been found to suppress clinical symptoms in mouse
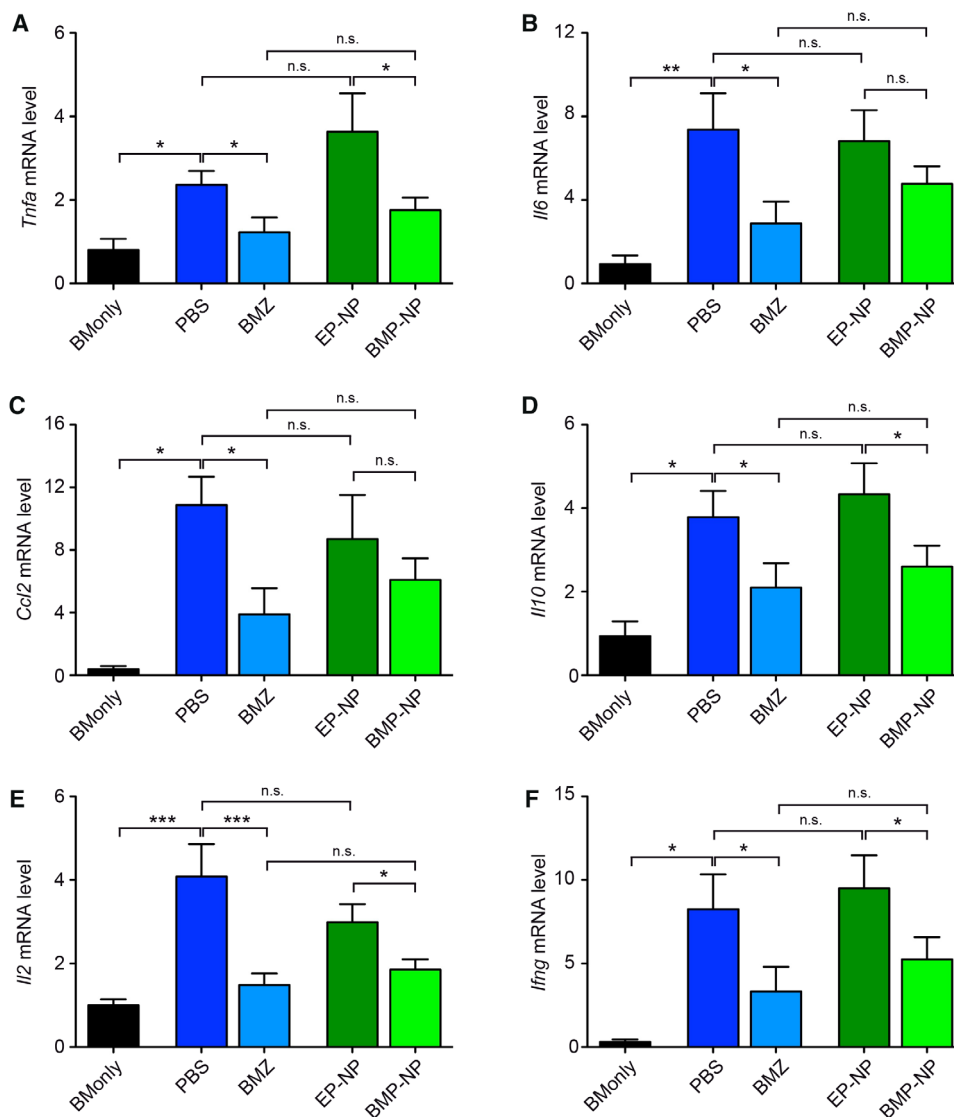
Figure 7. Impact of GCs on gene expression of inflammatory mediators in the small intestine in the early phase of aGvHD. BALB/c mice were irradiated and then transplanted with BM and purified T cells from C57BL/6 mice. Treatment with GCs (BMZ or BMP-NP) or vehicles (PBS or EP-NP) was performed at days 3, 4, and 5; mice receiving only BM cells served as a control. RNA was isolated from the small intestine at day 6 and analyzed by quantitative RT-PCR. Relative mRNA levels of (A) *Tnfa*, (B) *Il6*, (C) *Ccl2*, (D) *Il10*, (E) *Il2*, and (F) *Ifng* were calculated by normalization to the housekeeping gene *Hprt*. Gene expression in BMonly mice was arbitrarily set to 1. N = 6 (BMonly), N = 7–8 (PBS), N = 7–11 (BMZ), N = 7–10 (EP-NP), N = 8–12 (BMP-NP); data were pooled from three experiments. Values are depicted as the mean ± SEM and were analyzed using a one-way ANOVA followed by a Newman–Keuls multiple comparison test. Levels of significance are $^*p < 0.05$; $^{**}p < 0.01$; $^{***}p < 0.001$; n.s., non-significant. The indicated sample size (N) refers to the total number of individual mice analyzed in each experimental group.

models of MS, lupus erythematosus, and ulcerative colitis [16,20,21]. Only little experience with using nanoformulations, however, has been made in the context of aGvHD. Delivery of cyclosporine A with iron nanoparticles improved the survival of mice after aGvHD induction to a similar extent as the free drug [28]. Treatment of aGvHD with a dexamethasone palmitate emulsion that is preferentially taken up by macrophages reduced clinical symptoms and led to longer survival times compared to the application of free dexamethasone [29]. It is noteworthy that the latter finding is in line with our own observation that selectively targeting GCs to macrophages by using IOH-NPs prolongs survival after aGvHD induction at least as efficiently

as the free drug. Hence, there is good evidence that modulating myeloid cell activity suffices to mitigate aGvHD symptoms. Since T cell activity is at least partially retained here, the GvL effect should be improved as it was the case in our study.

IOH-NPs are a new type of nanoformulation characterized by a high drug load, i.e., 74 wt% of BMP per nanoparticle, easy synthesis in water, and good tolerability of all constituents [30,31]. They are preferentially taken up by macrophages, less efficiently by fibroblasts, epithelial cells, and myoblasts, and almost not by T and B cells [22,23]. After intraperitoneal injection into mice, IOH-NPs are disseminated to abdominal organs including the small
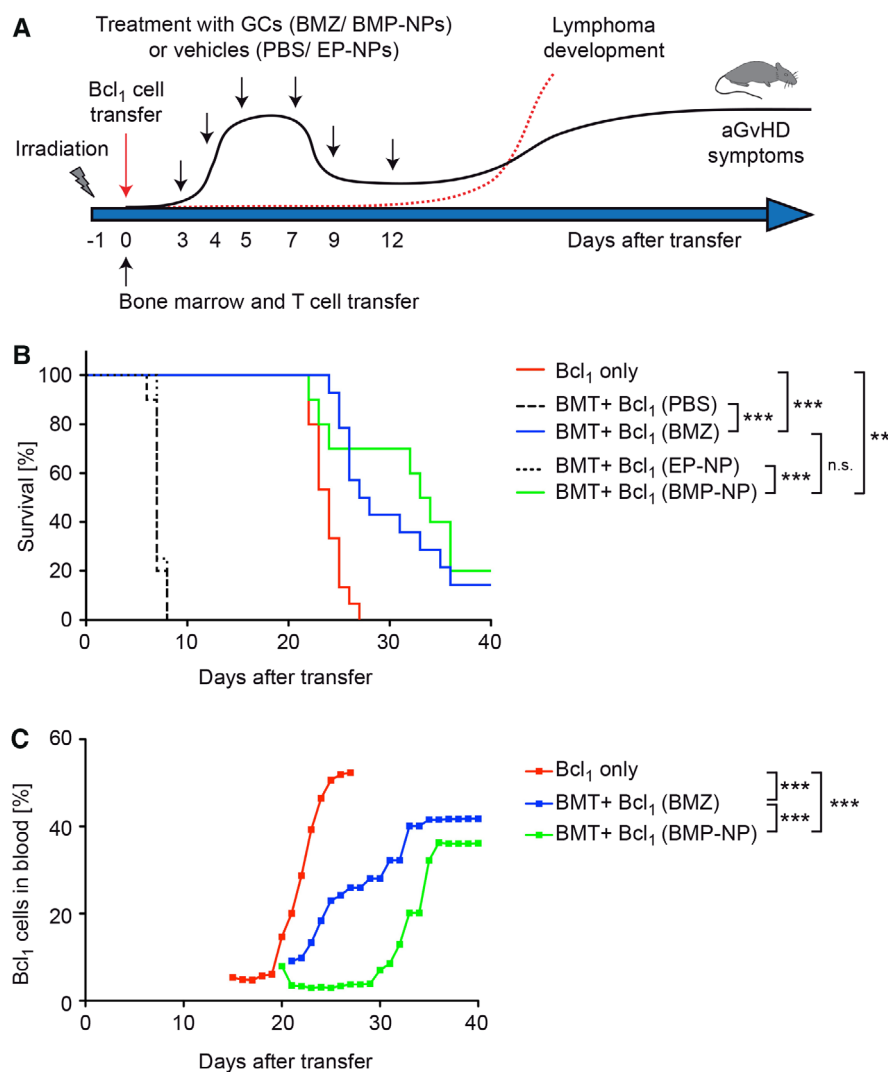
Figure 8. Mortality and lymphomagenesis in a combined aGvHD/GvL mouse model after GC treatment. BALB/c mice were irradiated and adoptively transferred with Bcl_1 lymphoma cells. Then mice were transplanted with BM and purified T cells from C57BL/6 mice to induce aGvHD. Treatment with GCs (BMZ or BMP-NP) or vehicles (PBS or EP-NP) was performed at days 3, 4, 5, 7, 9, and 12. One group of mice was only transferred with Bcl_1 cells. (A) Schematic representation of the aGvHD/GvL experiment and the therapeutic regimen. (B) Survival of mice based on the applying ethical criteria was monitored for 40 days. N = 15 (Bcl_1 only), N = 10 (PBS), N = 14 (BMZ), N = 4 (EP-NP), N = 10 (BMP-NP); data were pooled from up to five experiments. Statistical analysis was done by Log-rank Mantel–Cox test. (C) Average percentage of Bcl_1 cells in the peripheral blood as determined by flow cytometric analysis of λ light chain surface expression (only mice that did not decease from aGvHD symptoms were considered in the graph). N = 15 (Bcl_1 only), N = 7 (BMZ), N = 6 (BMP-NP); pooled from five experiments. Statistical analysis was performed by one-way ANOVA followed by a Newman–Keuls multiple comparison test. Levels of significance are $*p < 0.05$; $**p < 0.01$; $***p < 0.001$; n.s., non-significant. The indicated sample size (N) refers to the total number of individual mice analyzed in each experimental group. The gating strategy used for the analysis of Bcl_1 cells in the blood is illustrated in Supporting Information Fig. 3.

intestine, where they are particularly engulfed by macrophages [23]. It can be expected that the targeting of IOH-NPs to aGvHD target tissues is additionally fostered by the ELVIS mechanism, which is known to cause an accumulation of nanomaterial in inflamed tissues [14,15]. IOH-NPs should therefore easily reach the inflamed small intestine and exert their effects locally. In fact, this is exactly what we observed in our study. Regardless of the drug formulation, GCs ameliorated clinical symptoms and tissue damage, but the mechanism by which this was achieved was different. Free BMZ reduced immune cell infiltration into the small intestine and altered the composition of the major myeloid cell subsets. In particular, the accumulation of inflammatory macrophages was prevented by free BMZ, which could either be explained by their reduced trafficking to the small intestine or a polarization of newly recruited macrophages toward an anti-inflammatory phenotype in situ. Importantly, BMP-NPs had no effect on these features, suggesting that their therapeutic efficacy must rely on a different mechanism. In contrast to the above-mentioned observations, BMZ and BMP-NPs were largely undistinguishable in regard to their local inhibitory effects on

cytokine and chemokine gene expression in the small intestine. Our results therefore indicate that the suppression of myeloid cells in aGvHD target organs probably suffices to mitigate the disease without the need of any systemic effects or a direct repression of T cells. The relevance of this conclusion goes beyond the study at hand as it strongly entails new efforts to target myeloid cells in aGvHD instead of T cells as it is the case for most currently employed therapies.

Successful therapeutic intervention after HSCT should not only prevent the development of aGvHD but also retain the GvL activity of the allogeneic T cells contained in the graft, and thus prevent a relapse of the underlying disease. None of the existing aGvHD therapies including GCs currently fulfill this requirement well. GCs repress the migration, adhesion, and cytokine expression of T cells and induce their apoptosis via the intrinsic pathway [32–34]. All these effects contribute to the repression of aGvHD, but they also compromise the cytotoxic activity of the T cells needed to destroy residual malignant cells. Hence, the beneficial and deleterious effects of free GCs cannot be separated. This is different for GC nanoformulations such as IOH-NPs that selectively act on myeloid
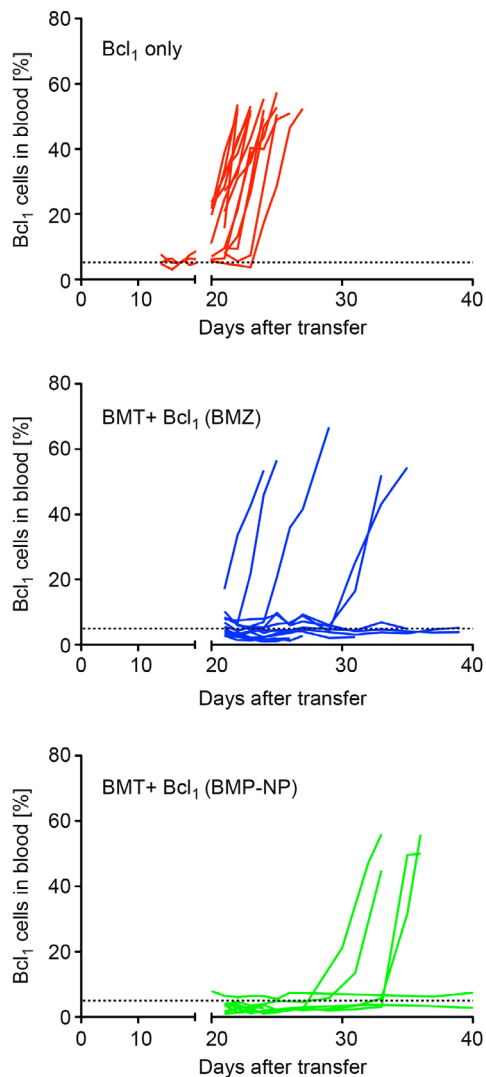
Figure 9. Bcl_1 lymphoma cell expansion in individual mice in a combined aGvHD/GvL model after GC treatment. BALB/c mice were irradiated and adoptively transferred with Bcl_1 lymphoma cells. Then, mice were also transplanted with BM and purified T cells from C57BL/6 mice to induce aGvHD. BMZ or BMP-NP treatment was performed at days 3, 4, 5, 7, 9, and 12. One group of mice was only transferred with Bcl_1 cells. Data refer to the same experiments as depicted in Fig. 8. The percentage of Bcl_1 cells in the peripheral blood was determined by flow cytometric analysis of λ light chain surface expression and is separately depicted for each individual mouse. N = 15 (Bcl_1 only), N = 14 (BMZ), N = 10 (BMP-NP); pooled from five experiments. The dashed line refers to the percentage with which B cells in mice naturally express the λ light chain. The indicated sample size (N) refers to the total number of individual mice analyzed in each experimental group.

cells. According to our data, aGvHD is equally well suppressed by BMP-NPs and free BMZ while it took longer until lymphoma cells accumulated in the peripheral blood of mice treated with BMP-NPs. Although our findings indicate that the use of IOH-NPs for GC delivery enhances the GvL effect of the graft, the incidence of lymphomagenesis remained largely unaltered. Furthermore, only a few mice survived beyond day 35. In this context, it is noteworthy that GCs were only given for a relatively short period of

time and that the therapeutic effect might be more sustained if the treatment was extended. In addition, a higher GC dose could result in longer survival times as we have previously shown in a mouse EAE model that therapeutic efficacy is dose-dependent [34]. Irrespective of these caveats, the study at hand provides first evidence that GCs delivered via IOH-NPs retain their therapeutic activity in aGvHD while improving the GvL activity of the graft.

Materials and methods

Preparation of inorganic–organic hybrid nanoparticles

$[ZrO]^{2+}[(BMP)_{0.9}(FMN)_{0.1}]^{2-}$ IOH-NPs (designated BMP-NPs) and as a vehicle control $[ZrO]^{2+}[(HPO_4)_{0.9}(FMN)_{0.1}]^{2-}$ IOH-NPs without the drug (designated EP-NPs) were prepared essentially as described [30]. Synthesis was achieved by admixing a solution of $ZrOCl_2 \times 8H_2O$ in H_2O to a solution of either $Na_2(BMP)$ or $Na_2(HPO_4)$ together with sodium riboflavin-5'-mono-phosphate dihydrate (Na(HFMN) in H_2O). Thereafter, nucleated IOH-NPs were separated by centrifugation. BMP-NPs were redispersed in H_2O at a concentration of 2.4–3.2 mg/mL, which corresponds to 4.2–5.5 mM. Since EP-NPs were produced at the same molarity as BMP-NPs, their mass concentration was accordingly lower.

Quality control of IOH-NP preparations

To unveil a potential contamination of the nanoparticles by endotoxins, mice were daily injected with 100 μL BMP-NPs or PBS i.p. for 2 wks and TNF-α and IL-6 serum levels were analyzed by ELISA. The lack of any inflammatory response confirmed that the nanoparticle preparations were free of endotoxins (Supporting Information Fig. 4A and B).

Animal experimentation

C57BL/6 and BALB/c WT mice were purchased from Janvier Labs (St. Berthevin, France), whereas GR^{flox} ($Nr3c1^{tm2GSc}$) and GR^{lysM} ($Nr3c1^{tm2GSc}Lyz2^{tm1(Cre)Ifo}$) mice on a BALB/c background [9] were bred in our animal facilities at the University Medical Center Göttingen. All mice were kept in individually ventilated cages under specific-pathogen-free conditions, supplied with food and water ad libitum, and used at an age of 8–12 weeks. All experiments were conducted according to Lower Saxony state regulations for animal experimentation and approved by the responsible authority (*Niedersächsisches Landesamt für Verbraucherschutz und Lebensmittelsicherheit*).

Totally MHC mismatched aGvHD mouse model

Bone marrow (BM) was prepared from the long bones of C57BL/6 mice followed by depleting T cells using the EasySep^{TM} Positive Selection Mouse CD90.2 Kit II (StemCell Technologies, Grenoble,

France). Splenic T cells were purified with the help of the EasySep™ Negative Selection Mouse T Cell Isolation Kit (StemCell Technologies) after passing the organ through a 40 µm cell strainer. BALB/c mice of the different genotypes were irradiated with a dose of 8.5 Gy using an X-Ray source operated at 200 kV, 15 mA and 0.5-mm Cu filtration. On the next day, 1×10^7 BM cells and 2×10^6 T cells were injected via the tail vein (BMT cell transfer) to induce aGvHD [10]. Mice receiving only BM cells served as a control. Neomycin (25 µg/mL) was added to the drinking water for up to 3 wks starting 1 day before irradiation to prevent infections. Clinical symptoms were monitored based on five parameters: posture, activity, fur ruffling, diarrhea, and weight loss, and depending on severity, each parameter was assigned a score between 0 and 2. Mice were sacrificed by CO_2 inhalation to collect organs for analysis, or when they reached the abort criteria. Body temperature was measured using a BIO-TK9882 thermometer equipped with a BIO-BRET-3 rectal probe (Bioseb, Vitrolles, France).

Combined aGvHD/GvL mouse model

Bcl_1 lymphoma cells [35–37] were freshly thawed and injected into irradiated BALB/c mice at a dose of 3000 cells per mouse via the tail vein. 4 h later, aGvHD was induced and clinical symptoms were monitored as described above. Lymphoma development was determined by assessing the percentage of Bcl_1 cells in the blood by flow cytometry starting at day 15. To this end, a drop of blood was collected from the tail vein and stained with a monoclonal antibody detecting the λ light chain of the BCR as outlined below. Mice were sacrificed when reaching the abort criteria defined for clinical aGvHD symptoms or once the percentage of Bcl_1 cells in the peripheral blood exceeded 50% of all lymphocytes.

Glucocorticoid therapy of aGvHD

Different treatment protocols were applied depending on the experimental setup. In short-term experiments, GCs were injected i.p. at day 3, 4 and 5 and the mice were sacrificed at day 6. In long-term experiments lasting 40–50 days, the treatment was done at day 3, 4, 5, 7, 9 and 12. Betamethasone (Celestan®, Merck, Darmstadt, Germany; designated BMZ) was applied at a concentration of 10 mg/kg body weight, and a similar volume of PBS served as a control. BMP-NPs were administered at a dose corresponding to 10 mg/kg BMZ. In this case, a similar volume of EP-NPs (empty IOH-NPs without the drug) was injected as a vehicle control, containing the same amount of zirconyl ($[ZrO]^{2+}$), and largely the same number of particles as BMP-NPs.

Histology

Biopsies of the small intestine were obtained from the central part of the jejunum and fixed in 4% PFA (Carl Roth, Karlsruhe, Germany) for 48 h. Following dehydration and embedding in paraffin, 2 µm sections were prepared and stained with H&E or by Periodic acid-Schiff (PAS) reaction following standard procedures. A Leica Axio Scope A1 microscope (Wetzlar, Germany) was used to acquire photomicrographs. Evaluation of tissue damage was done in a blinded manner and based on four criteria (villous blunting/flattening, number of apoptotic cells, grade of inflammation, and edema) as described previously [38]. To this end, 10 fields per section were analyzed at 200× magnification followed by calculating the total histopathological score. Goblet cell numbers were determined by evaluating 10 fields per section at 400× magnification.

Immunohistochemistry

Detection of T cells and myeloid cells was achieved by incubating 2 µm tissue sections with EnVision Flex Target Retrival Solution, Low pH (Dako Agilent Technologies, Santa Clara, CA) followed by staining for 30 min at room temperature with primary antibodies recognizing CD3 (1:2000; Santa Cruz Biotechnology) or CD68 (1:200; Abcam, Cambridge, UK). Sites of immunoreactivity were visualized by using polymeric secondary antibodies coupled to HRP (ImmPRESS HRP Polymer Detection Kit; Vector Laboratories, Burlingame, CA) and DAB (Dako Agilent Technologies). Photomicrographs were acquired with a Leica Axio Scope A1 microscope after counterstaining the sections with hematoxylin. Quantification of CD3+ cells was achieved by counting stained cells in tissue sections at 200× magnification directly under the microscope. To enumerate CD68+ cells, 10 pictures per tissue section were taken at 200× magnification, and the stained area covered by CD68+ cells was determined with the help of ImageJ software (https://imagej.nih.gov/ij/).

Isolation of lamina propria cells

The small intestine was flushed with PBS, opened longitudinally, and incubated on ice in PBS containing 3 mM DTT and 60 mM EDTA (Carl Roth). Subsequently, the epithelial cell layer was removed by repeated vigorous shaking as described previously [39]. The remaining tissue was washed with RPMI medium containing 10% FCS and 1% penicillin/streptomycin (Thermo Fisher Scientific), cut into small pieces and digested for 30 min at 37°C by using 100 U/mL collagenase II, 100 U/mL collagenase 1A, and 50 U/mL DNaseII type V (all from Sigma–Aldrich, Taufkirchen, Germany). Single-cell suspensions were obtained by passing the digested tissue through a 40 µm cell strainer and used for analysis by flow cytometry.

Flow cytometry

Cells were resuspended in PBS supplemented with 0.1% BSA and 0.01% NaN_3 and stained with monoclonal antibodies conjugated with different fluorochromes (BioLegend, Uithoorn, the Netherlands; clone name in brackets): anti-CD3 (17A2), anti-CD4 (RM4-5), anti-CD8 (53-6.7), anti-CD11b (M1/70), anti-Ly6G (1A8),

anti-Ly6C (HK1.4), and anti-Igλ (RML-42). An FcR blockade was performed by using TruStain fcX (anti-mouse CD16/32; clone: 93) prior to the antibody staining. To remove erythrocytes from blood samples, they were treated with OptiLyse B (Beckman Coulter). Data were acquired with an FACS Canto II flow cytometer (BD Bioscience, Heidelberg, Germany) and analyzed with FlowJo® software (Tree Star, Ashland/OR, USA). Gating strategies used for the analysis of lymphocytes and myeloid cells in the lamina propria of the inflamed instestine and Bcl_1 lymphoma cells in the blood are illustrated in Supporting Information Figs. 1–3. The employed method adheres to the "Guidelines for the use of flow cytometry and cell sorting in immunological studies" [40].

ELISA and quantitative RT-PCR

Serum was prepared from blood samples obtained by cardiac puncture. IL-6, TNF-α, IFN-γ, and CCL2 levels were determined by ELISA using commercially available kits according to the manufacturer's instructions (BioLegend or Affymetrix eBioscience, Frankfurt, Germany). Total RNA was prepared from tissue samples with the help of the RNeasy Mini Kit (Qiagen, Hilden, Germany) and reverse transcribed into cDNA using the iScript Kit (Bio-Rad, Munich, Germany). Quantitative RT-PCR employing the SYBR green mastermix was performed on an ABI 7500 instrument (both Applied Biosystems, Darmstadt, Germany). Gene expression was normalized to the mRNA levels of *Hprt* and evaluated using the ΔΔCt method. All primers were synthesized by Metabion (Planegg, Germany); sequences are available upon request.

Statistical analysis

Kaplan–Meier survival curves were analyzed with the Log-rank Mantel–Cox test; in all other cases, a one-way ANOVA followed by a Newman–Keuls multiple comparison test was used. A Grubbs' test was employed to identify outliers in data sets. Statistical analyses were done with Prism® software (GraphPad Software, San Diego, CA). Levels of significance: $*p < 0.05$, $**p < 0.01$, $***p < 0.001$, n.s., non-significant.

Author contribution: T.K.K. performed experiments and analyzed data; H.L. performed experiments and analyzed data; L.R. performed experiments; S.D.R. supervised experiments and provided methodology; H.B. supervised histological analyses; C.F. supervised nanoparticle synthesis; H.R. designed the project, supervised experiments, analyzed data, and wrote the manuscript

Conflict of interest: The authors have declared that no commercial or financial conflict of interest exists.

References

1 **Zeiser, R. and Blazar, B. R.**, Acute graft-versus-host disease - biologic process, prevention, and therapy. *N. Engl. J. Med.* 2017. **377**: 2167–2179.

2 **Hill, L., Alousi, A., Kebriaei, P., Mehta, R., Rezvani, K. and Shpall, E.**, New and emerging therapies for acute and chronic graft versus host disease. *Ther. Adv. Hematol.* 2018. **9**: 21–46.

3 **Pidala, J., Kim, J., Kharfan-Dabaja, M. A., Nishihori, T., Field, T., Perkins, J., Perez, L. et al.**, Dysglycemia following glucocorticoid therapy for acute graft-versus-host disease adversely affects transplantation outcomes. *Biol. Blood Marrow Transplant.* 2011. **17**: 239–248.

4 **Waddell, D. S., Baehr, L. M., van den Brandt, J., Johnsen, S. A., Reichardt, H. M., Furlow, J. D. and Bodine, S. C.**, The glucocorticoid receptor and FOXO1 synergistically activate the skeletal muscle atrophy-associated MuRF1 gene. *Am. J. Physiol.* 2008. **295**: E785-797.

5 **Rauch, A., Seitz, S., Baschant, U., Schilling, A. F., Illing, A., Stride, B., Kirilov, M. et al.**, Glucocorticoids suppress bone formation by attenuating osteoblast differentiation via the monomeric glucocorticoid receptor. *Cell Metab.* 2010. **11**: 517–531.

6 **Ferrara, J. L., Levine, J. E., Reddy, P. and Holler, E.**, Graft-versus-host disease. *Lancet* 2009. **373**: 1550–1561.

7 **Shlomchik, W. D.**, Graft-versus-host disease. *Nat. Rev. Immunol.* 2007. **7**: 340–352.

8 **Martin, P. J., Rizzo, J. D., Wingard, J. R., Ballen, K., Curtin, P. T., Cutler, C., Litzow, M. R. et al.**, First- and second-line systemic treatment of acute graft-versus-host disease: recommendations of the American Society of Blood and Marrow Transplantation. *Biol. Blood Marrow Transplant.* 2012. **18**: 1150–1163.

9 **Baake, T., Jörß, K., Suennemann, J., Roßmann, L., Bohnenberger, H., Tuckermann, J. P., Reichardt, H. M. et al.**, The glucocorticoid receptor in recipient cells keeps cytokine secretion in acute graft-versus-host disease at bay. *Oncotarget* 2018. **9**: 15437–15450.

10 **Theiss-Suennemann, J., Jörß, K., Messmann, J. J., Reichardt, S. D., Montes-Cobos, E., Lühder, F., Tuckermann, J. P. et al.**, Glucocorticoids attenuate acute graft-versus-host disease by suppressing the cytotoxic capacity of CD8(+) T cells. *J. Pathol.* 2015. **235**: 646–655.

11 **Li, H., Kaiser, T. K., Borschiwer, M., Bohnenberger, H., Reichardt, S. D., Lühder, F., Walter, L. et al.**, Glucocorticoid resistance of allogeneic T cells alters the gene expression profile in the inflamed small intestine of mice suffering from acute graft-versus-host disease. *J. Steroid Biochem. Mol. Biol.* 2019: 105485.

12 **Bouazzaoui, A., Spacenko, E., Mueller, G., Huber, E., Schubert, T., Holler, E., Andreesen, R. et al.**, Steroid treatment alters adhesion molecule and chemokine expression in experimental acute graft-vs.-host disease of the intestinal tract. *Exp. Hematol.* 2011. **39**: 238–249.e231.

13 **Lühder, F. and Reichardt, H. M.**, Novel drug delivery systems tailored for improved administration of glucocorticoids. *Int. J. Mol. Sci.* 2017. **18**.

14 **Kopecek, J.**, Polymer-drug conjugates: origins, progress to date and future directions. *Adv. Drug Deliver. Rev.* 2013. **65**: 49–59.

15 Yuan, F., Quan, L. D., Cui, L., Goldring, S. R. and Wang, D., Development of macromolecular prodrug for rheumatoid arthritis. *Adv. Drug Deliver. Rev.* 2012. **64**: 1205–1219.

16 Schweingruber, N., Haine, A., Tiede, K., Karabinskaya, A., van den Brandt, J., Wüst, S., Metselaar, J. M. et al., Liposomal encapsulation of glucocorticoids alters their mode of action in the treatment of experimental autoimmune encephalomyelitis. *J. Immunol.* 2011. **187**: 4310–4318.

17 Schmidt, J., Metselaar, J. M., Wauben, M. H., Toyka, K. V., Storm, G. and Gold, R., Drug targeting by long-circulating liposomal glucocorticosteroids increases therapeutic efficacy in a model of multiple sclerosis. *Brain* 2003. **126**: 1895–1904.

18 Zhao, C. Y., Fan, T. T., Yang, Y., Wu, M. L., Li, L., Zhou, Z., Jian, Y. L. et al., Preparation, macrophages targeting delivery and anti-inflammatory study of pentapeptide grafted nanostructured lipid carriers. *Int. J. Pharmaceut.* 2013. **450**: 11–20.

19 Ren, K., Dusad, A., Yuan, F., Yuan, H. J., Purdue, P. E., Fehringer, E. V., Garvin, K. L. et al., Macromolecular prodrug of dexamethasone prevents particle-induced peri-implant osteolysis with reduced systemic side effects. *J. Control Release* 2014. **175**: 1–9.

20 Ren, K., Yuan, H. J., Zhang, Y. J., Wei, X. and Wang, D., Macromolecular glucocorticoid prodrug improves the treatment of dextran sulfate sodium-induced mice ulcerative colitis. *Clin. Immunol.* 2015. **160**: 71–81.

21 Jia, Z., Wang, X., Wei, X., Zhao, G., Foster, K. W., Qiu, F., Gao, Y. et al., Micelle-forming dexamethasone prodrug attenuates nephritis in lupus-prone mice without apparent glucocorticoid side effects. *ACS Nano* 2018. **12**: 7663–7681.

22 Montes-Cobos, E., Ring, S., Fischer, H. J., Heck, J., Strauss, J., Schwaninger, M., Reichardt, S. D. et al., Targeted delivery of glucocorticoids to macrophages in a mouse model of multiple sclerosis using inorganic-organic hybrid nanoparticles. *J. Control Release* 2017. **245**: 157–169.

23 Kaiser, T. K., Khorenko, M., Moussavi, A., Engelke, M., Boretius, S., Feldmann, C. and Reichardt, H. M., Highly selective organ distribution and cellular uptake of inorganic-organic hybrid nanoparticles customized for the targeted delivery of glucocorticoids. *J. Control Release* 2020. **319**: 360–370.

24 Lee, S. J., Zahrieh, D., Agura, E., MacMillan, M. L., Maziarz, R. T., McCarthy, P. L., Jr., Ho, V. T. et al., Effect of up-front daclizumab when combined with steroids for the treatment of acute graft-versus-host disease: results of a randomized trial. *Blood* 2004. **104**: 1559–1564.

25 Waldmann, T. A. and O'Shea, J., The use of antibodies against the IL-2 receptor in transplantation. *Curr. Opin. Immunol.* 1998. **10**: 507–512.

26 Rech, A. J., Mick, R., Martin, S., Recio, A., Aqui, N. A., Powell, D. J., Jr., Colligon, T. A. et al., CD25 blockade depletes and selectively reprograms regulatory T cells in concert with immunotherapy in cancer patients. *Sci. Transl. Med.* 2012. **4**: 134ra162.

27 Hoffmann, P., Ermann, J., Edinger, M., Fathman, C. G. and Strober, S., Donor-type CD4(+)CD25(+) regulatory T cells suppress lethal acute graft-versus-host disease after allogeneic bone marrow transplantation. *J. Exp. Med.* 2002. **196**: 389–399.

28 Cheng, J., Zhou, Y., Chen, B., Wang, J., Xia, G., Jin, N., Ding, J. et al., Prevention of acute graft-versus-host disease by magnetic nanoparticles of Fe(3)O(4) combined with cyclosporin A in murine models. *Int. J. Nanomed.* 2011. **6**: 2183–2189.

29 Nishiwaki, S., Nakayama, T., Murata, M., Nishida, T., Terakura, S., Saito, S., Kato, T. et al., Dexamethasone palmitate ameliorates macrophages-rich graft-versus-host disease by inhibiting macrophage functions. *PLoS One* 2014. **9**: e96252.

30 Heck, J. G., Napp, J., Simonato, S., Mollmer, J., Lange, M., Reichardt, H. M., Staudt, R. et al., Multifunctional phosphate-based inorganic-organic hybrid nanoparticles. *J. Am. Chem. Soc.* 2015. **137**: 7329–7336.

31 Neumeier, B. L., Khorenko, M., Alves, F., Goldmann, O., Napp, J., Schepers, U., Reichardt, H. M. et al., Fluorescent inorganic-organic hybrid nanoparticles. *ChemNanoMat* 2019. **5**: 24–45.

32 Schweingruber, N., Fischer, H. J., Fischer, L., van den Brandt, J., Karabinskaya, A., Labi, V., Villunger, A. et al., Chemokine-mediated redirection of T cells constitutes a critical mechanism of glucocorticoid therapy in autoimmune CNS responses. *Acta Neuropathol.* 2014. **127**: 713–729.

33 Wang, D., Müller, N., McPherson, K. G. and Reichardt, H. M., Glucocorticoids engage different signal transduction pathways to induce apoptosis in thymocytes and mature T cells. *J. Immunol.* 2006. **176**: 1695–1702.

34 Wüst, S., van den Brandt, J., Tischner, D., Kleiman, A., Tuckermann, J. P., Gold, R., Lühder, F. et al., Peripheral T cells are the therapeutic targets of glucocorticoids in experimental autoimmune encephalomyelitis. *J. Immunol.* 2008. **180**: 8434–8443.

35 Warnke, R. A., Slavin, S., Coffman, R. L., Butcher, E. C., Knapp, M. R., Strober, S. and Weissman, I. L., The pathology and homing of a transplantable murine B cell leukemia (BCL1). *J. Immunol.* 1979. **123**: 1181–1188.

36 Tutt, A. L., Stevenson, F. K., Slavin, S. and Stevenson, G. T., Secretion of idiotypic IgM by the mouse B-cell leukaemia (BCL1) occurs spontaneously in vitro and in vivo. *Immunology* 1985. **55**: 59–63.

37 Beyersdorf, N., Ding, X., Hünig, T. and Kerkau, T., Superagonistic CD28 stimulation of allogeneic T cells protects from acute graft-versus-host disease. *Blood* 2009. **114**: 4575–4582.

38 Kaplan, D. H., Anderson, B. E., McNiff, J. M., Jain, D., Shlomchik, M. J. and Shlomchik, W. D., Target antigens determine graft-versus-host disease phenotype. *J. Immunol.* 2004. **173**: 5467–5475.

39 Meers, G. K., Bohnenberger, H., Reichardt, H. M., Lühder, F. and Reichardt, S. D., Impaired resolution of DSS-induced colitis in mice lacking the glucocorticoid receptor in myeloid cells. *PLoS One* 2018. **13**: e0190846.

40 Cossarizza, A., Chang, H. D., Radbruch, A., Acs, A., Adam, D., Adam-Klages, S., Agace, W. W. et al., Guidelines for the use of flow cytometry and cell sorting in immunological studies (second edition). *Eur. J. Immunol.* 2019. **49**: 1457–1973.

Full correspondence: Prof. Holger M. Reichardt, Institute for Cellular and Molecular, Immunology, University Medical Center Göttingen, Humboldtallee 34, 37073 Göttingen, Germany
e-mail: hreichardt@med.uni-goettingen.de

Current address: Laura Roßmann, Division of Immunology, Paul-Ehrlich-Institute, Langen, 63225, Germany.